

# Frictional cooling of positively charged particles

Daniel Greenwald<sup>1a</sup>, Allen Caldwell<sup>a</sup>

<sup>a</sup>*Max Planck Institute for Physics, Munich, Germany*

---

## Abstract

One of the focuses of research and development towards the construction of a muon collider is muon beam preparation. Simulation of frictional cooling shows that it can achieve the desired emittance reduction to produce high-luminosity muon beams. We show that for positively charged particles, charge exchange interactions necessitate significant changes to schemes previously developed for negatively charged particles. We also demonstrate that foil-based schemes are not viable for positive particles.

*Keywords:* Frictional Cooling, Effective Charge, Charge Exchange Process, Muon Collider

---

## 1. Introduction

One of the focuses of research and development towards the construction of a muon collider is muon beam creation and preparation. The short lifetime of the muon necessitates preparation of a muon beam on time scales shorter than a microsecond. To achieve luminosities on the order of  $10^{34} \text{ cm}^{-2} \cdot \text{s}^{-1}$  as in the schemes of [1, 2, 3], requires a reduction of beam emittance—known as beam cooling—by six orders of magnitude.

Simulations of frictional cooling [4] show that it can achieve the desired emittance reduction and potentially produce high-luminosity muon beams [3]. Previous work on frictional cooling, including both simulation and experiment [5], focused on cooling  $\mu^-$  beams and assumed the cooling mechanism would be identical for  $\mu^+$  beams. However, positively charged particles, unlike negatively charged ones, participate in charge exchange processes, and this greatly alters their cooling. In this paper, we present calculations and simulations of the effects of charge exchange processes on the frictional cooling of positive particles. We also show that previous simulations of foil-based schemes are invalid for positive particles, and rule out the viability of such schemes.

---

<sup>1</sup>Corresponding author, deg@mpp.mpg.de

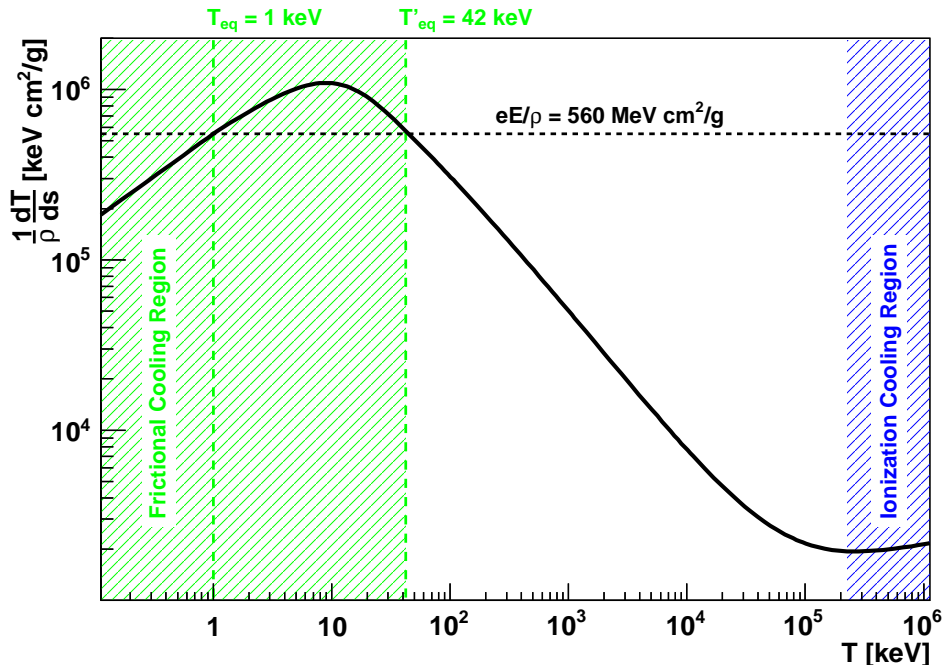


Figure 1: Stopping power of helium on  $\mu^+$  (velocity scaled from [6]) and the acceleration power of an electric field of fixed strength  $E$  for a particle of constant unit charge as functions of particle energy  $T$ .

## 2. Frictional Cooling

Frictional cooling reduces the energy spread and divergence of a beam by balancing retarding forces from interactions with a medium, with accelerating forces from an electric field to bring the beam to an equilibrium energy. Figure 1 shows the stopping power  $S = (1/\rho) dT/ds$ , where  $dT/ds$  is the energy loss per unit path length, and  $\rho$  is the medium density, for helium on  $\mu^+$  and the acceleration power  $(E/\rho)$  of an electric field of fixed strength  $E$  on a particle of constant unit charge. The stopping power is velocity scaled<sup>2</sup> [7] for  $\mu^+$  from the proton data given in [6]. The stopping power on  $\mu^-$  has a similar shape, though it is smaller in magnitude at energies below approximately 100 keV [8, 9]. When the accelerating power is larger than the stopping power, the particle is accelerated. When the reverse is true, the particle is decelerated. At the kinetic energies where the two powers are

---

<sup>2</sup>Except where noted, data for  $\mu^+$  interactions in this paper are velocity scaled from proton data.

$T_{\text{eq}}$	2.0	2.5	3.0	keV	
$dS/dT$	7.55	6.46	5.69	$\text{cm}^2/\text{mg}$	} $\mu^-$ in $\text{H}_2$
Total	0.60	0.69	0.83	keV	
Scattering	0.57	0.64	0.76	keV	
Straggling	0.18	0.27	0.34	keV	
Charge Exchange	0.07	0.11	0.17	keV	$\mu^+$ in He

Table 1: Energy spreads of frictionally cooled beams of  $\mu^-$  in  $\text{H}_2$  gas from [4] and  $\mu^+$  in He; and gradient of the stopping power of  $\text{H}_2$  on  $\mu^-$  from the parameterization in [8]

equal, particles are at an energy equilibrium. If the stopping power is greater than the accelerating power at energies above this equilibrium point and vice versa below it, then the point is stable and attractive.

For a particle of constant charge, two equilibrium points are created: a stable one ( $T_{\text{eq}}$  in figure 1) at an energy below that at which the stopping power peaks, and an unstable one at an energy above ( $T'_{\text{eq}}$ ). Particles with  $T < T'_{\text{eq}}$  will be brought to  $T_{\text{eq}}$ , defining the frictional cooling energy region.

Straggling of energy losses to the medium prevent a beam from becoming truly mono-energetic in a frictional cooling scheme, inducing a spread of the beam energy around  $T_{\text{eq}}$ . A study of the frictional cooling of  $\mu^-$  in [4] found that the spread of the energy distribution of a cooled beam is independent of the beam's initial spread and, as table 1 shows, decreases with increasing gradient of the stopping power. In the table, the gradient is calculated from the parameterization of the stopping power for hydrogen on  $\mu^-$  from [8], using the measured parameters given in the paper.

Such effects are shared by ionization cooling [10, 11], which operates at higher kinetic energies. However, in contrast to ionization cooling, frictional cooling, which operates at low kinetic energies, is greatly affected by nuclear scattering, which contributes to the spread in kinetic energies of the cooled beam to a larger extent than the straggling of energy losses. This is due to particles scattering away from the electric field direction, possibly even in directions opposed to that of the field; they are then slowed down and reaccelerated to the equilibrium energy in the direction of the field.

### 3. Low-Energy Stopping Processes

At high kinetic energies, a projectile slows down in a medium through excitation and ionization of the medium atoms. One can neglect the interactions with the nuclei of the medium and assume that a positively charged

projectile is stripped of all its electrons [12, 13]. Thus the stopping power of the medium for positive particles is the same as for negative ones. This is the energy region of ionization cooling, and the energy loss here is comparatively simpler to model than energy loss at low energies.

At low energies, projectiles slow down by Coloumbic interactions with both the nuclei and the electrons of the medium; furthermore the interactions of positively charged projectiles involve more than excitation and ionization, leading to a difference in the stopping powers for positive and negative projectiles.

Scattering of the projectile particle off of a nucleus results in a loss of energy and a change of direction. Though, as described above, nuclear scattering has the largest impact on the final energy spread of a cooled  $\mu^-$  beam, it is not the main mechanism of energy loss. The nuclear stopping power is orders of magnitude smaller than the electronic stopping power for all but the lowest kinetic energies [6].

### 3.1. Electronic Stopping

The interactions of the projectile<sup>3</sup> with the electrons of the stopping medium are the dominant mechanisms of energy loss. In the frictional-cooling energy region these interactions are the excitation and ionization of the medium atoms (X),

$$\mu^{(+)} + X \rightarrow \mu^{(+)} + X^* \quad (1a)$$

$$\mu^{(+)} + X^q \rightarrow \mu^{(+)} + X^{q+n} + ne^- \quad (1b)$$

and the capture and loss of an electron by the projectile,

$$\mu^{(+)} + X^q \rightarrow \mu^{(0)} + X^{q+1} \quad (1c)$$

$$\mu^{(0)} + X^q \rightarrow \mu^{(+)} + X^q + e^- \quad (1d)$$

$$\mu^{(0)} + X^q \rightarrow \mu^{(+)} + X^{q-1}, \quad (1e)$$

where we have introduced the notation  $\mu^{(q)}$  to represent charge states of  $\mu^+$  as an ion of muonium (Mu):

$$\begin{aligned} \mu^{(+)} &= \text{Mu}^+ = \mu^+, \\ \mu^{(0)} &= \text{Mu} = \mu^+e^-, \text{ and} \\ \mu^{(-)} &= \text{Mu}^- = \mu^+e^-e^-. \end{aligned} \quad (1f)$$

It is obvious that stopping of the neutral charge state plays a role in the stopping of the projectile. We must also consider processes (1a)–(1e) with

---

<sup>3</sup>The equations to follow are equally valid with  $\mu^+$  and Mu replaced by p and H.

the replacement of  $\mu^{(+)}$  by  $\mu^{(0)}$ , and  $\mu^{(0)}$  by  $\mu^{(-)}$ ; and processes involving the negative charge state: (1a) and (1b) with the replacement of  $\mu^{(+)}$  by  $\mu^{(-)}$ , and double electron capture and loss

$$\mu^{(+)} + X^q \rightarrow \mu^{(-)} + X^{q+2} \quad (1g)$$

$$\mu^{(-)} + X^q \rightarrow \mu^{(+)} + X^{q-2}. \quad (1h)$$

We write the cross sections for processes (1a)–(1h) for  $\mu^{(+)}$ ,  $\mu^{(0)}$ , and  $\mu^{(-)}$  with the notation  $\sigma_{qq'}(T)$ , denoting the total cross section for the interactions taking a muon of charge state  $q$  and energy  $T$  to a muon of charge state  $q'$  (accompanied by an energy loss). To be clear,  $q$  and  $q'$  refer to the charge state of the muonium ion (+, 0, −), not to the charge of the muon itself, which remains positive in these purely electromagnetic interactions.

The total stopping power of the projectile is the combination of the individual stopping powers of the different charge states,

$$\begin{aligned} S(T) &= \sum_q f^q(T) S^q(T) \\ &= f^+(T) S^+(T) + f^0(T) S^0(T) + f^-(T) S^-(T), \end{aligned} \quad (2)$$

where the  $f^q$  are the equilibrium charge state fractions [14], which are the solutions to

$$\frac{df^q}{dx} \propto \sum_{q'} (f^{q'} \sigma_{q'q} - f^q \sigma_{qq'}) = 0, \quad \forall q, \quad (3)$$

and

$$\sum_q f^q = 1. \quad (4)$$

Since the  $df^q/dx$  are taken at a fixed  $T$ , the  $f^q$  are functions of  $T$ . For the three-state system  $\{\mu^{(+)}, \mu^{(0)}, \mu^{(-)}\}$ , the equilibrium charge states are

$$f^q = A^q / \sum_{q'} A^{q'}, \quad (5a)$$

where

$$A^q \equiv \sum_{i \neq j \neq q} \sigma_{ij} \sigma_{jq} + \prod_{i \neq q} \sigma_{iq} \quad (5b)$$

By the nature of its measurement [6], the stopping power shown in figure 1 is the total stopping power; that is, the left-hand side of equation (2).

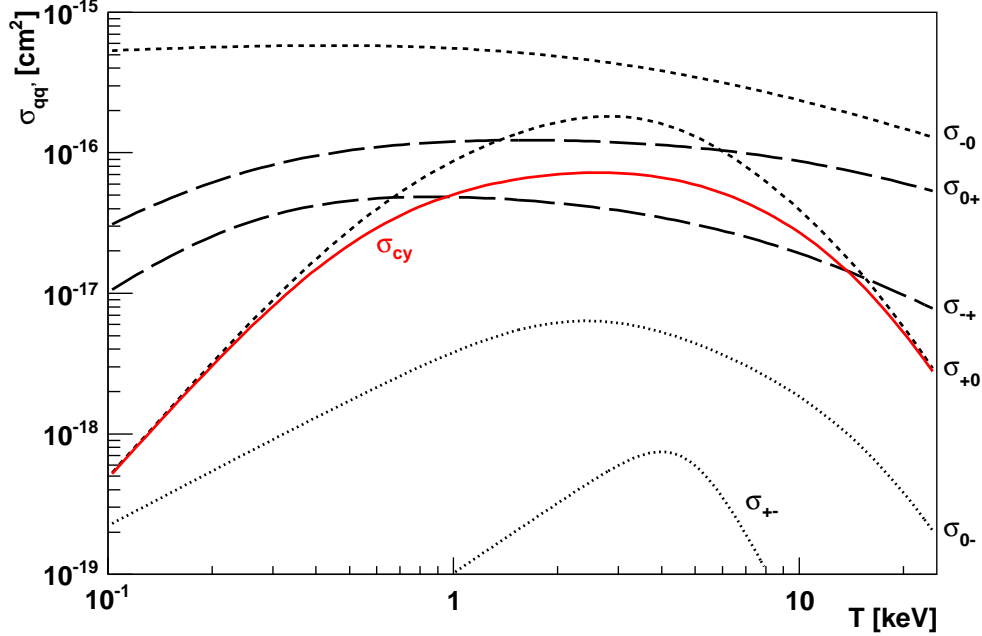


Figure 2: Charge exchange cross sections for  $\mu^+$  in helium, velocity scaled from proton cross sections in [15] resulting in final states with  $\mu^{(+)}$  (large dashes),  $\mu^{(0)}$  (small dashes), and  $\mu^{(-)}$  (dots). The two-state charge-change-cycle cross section is shown in solid red.

#### 4. Effective Charge

It is clear from section 3.1 that when traveling through matter,  $\mu^+$  spends some time as  $\text{Mu}$  and  $\text{Mu}^-$ . This changing of charge state will have a significant impact on the frictional cooling process, which involves the restoration of energy losses by an electric field according to  $qE$ .

Figure 2 shows the cross sections for the charge exchange processes of  $\mu^+$  in helium obtained by velocity scaling those for protons in [15]. The cross sections resulting in  $\mu^{(-)}$  charge states are orders of magnitude smaller than those taking  $\mu^{(-)}$  to  $\mu^{(+)}$  or  $\mu^{(0)}$ . So  $\mu^+$  traveling in helium (and in all the materials we will discuss) is nearly in a two-state system  $\{\mu^{(+)}, \mu^{(0)}\}$ . This simplifies the calculation of the equilibrium charge state fractions to

$$f^+ = \frac{\sigma_{0+}}{\sigma_{+0} + \sigma_{0+}} \quad \text{and} \quad f^0 = \frac{\sigma_{+0}}{\sigma_{+0} + \sigma_{0+}}. \quad (6)$$

The mean free path for one charge change cycle ( $\mu^{(+)} \rightarrow \mu^{(0)} \rightarrow \mu^{(+)}$ ) can be calculated from the mean free paths for the individual charge exchange

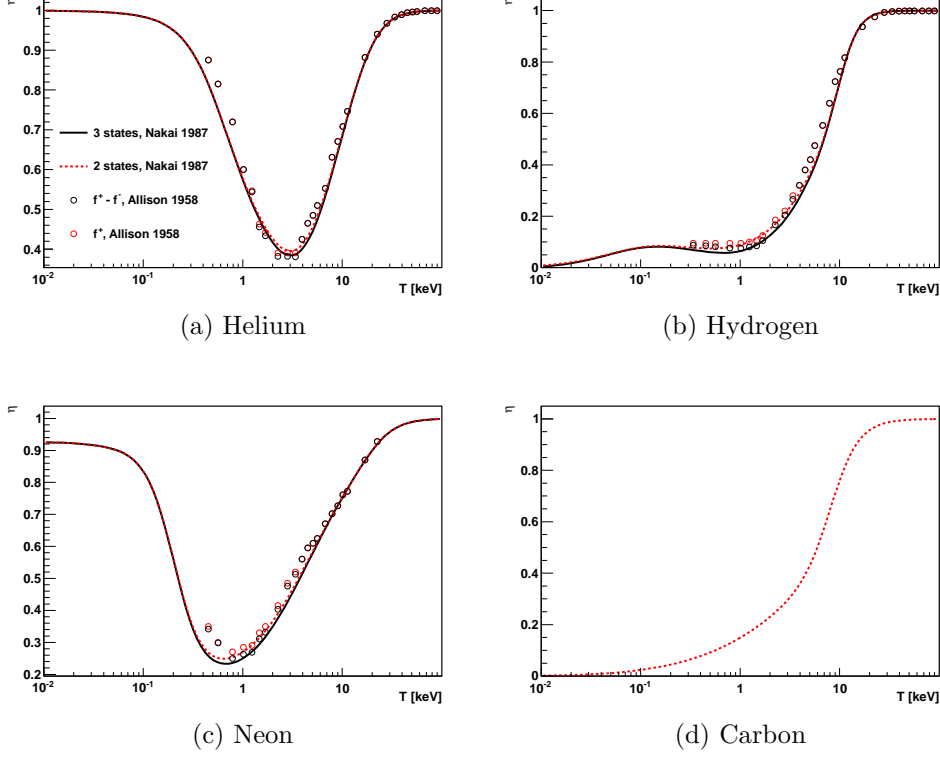


Figure 3: Effective charge (line) for  $\mu^+$  in He, H, Ne, and C for the three-state (solid black) and two-state (dashed red) systems. The data points show the equilibrium charge state fractions taken from [14].

processes,  $\lambda_{\text{cy}} = \lambda_{0+} + \lambda_{+0}$ . This yields a cross section for a charge exchange cycle to take place

$$\sigma_{\text{cy}} = \frac{\sigma_{+0} \sigma_{0+}}{\sigma_{+0} + \sigma_{0+}}, \quad (7)$$

which we show in figure 2. Since the charge exchange interactions take place over distances much shorter than the overall distance the muon travels in the frictional cooling scheme, we can approximate the charge of the  $\mu^+$  by an effective charge according to

$$\eta \equiv \sum_q q f^q. \quad (8)$$

Figure 3 shows the effective charges of  $\mu^+$  in helium, hydrogen, and neon for both the two-state ( $\eta_2$ ) and three-state ( $\eta_3$ ) systems calculated from the charge-exchange cross sections using empirical formulae from [16] fit to

measured values [15]. We also show  $\eta_2$  for carbon;  $\eta_3$  could not be calculated since the cross sections involving the negative charge state are unknown.

For comparison to the calculated effective charge, we show experimentally measured charge state fractions from [14] for helium, hydrogen, and neon:  $f^+$ , which is the same as  $\eta_2$ ; and  $(f^+ - f^-)$ , which is the same as  $\eta_3$ . The calculated effective charge matches very well with the measured data. As well, we see that  $\eta_2$  and  $\eta_3$  differ only minutely and only over a small range of energies. The negative charge state fraction contributes to the three-state effective charge at percent level and lower in all three gases.

It is important to note that helium and neon are the only materials in which the effective charge tends to a value of or near unity at low energies. In hydrogen and carbon (as well as water, oxygen, and nitrogen, and therefore air) the effective charge approaches zero at low energies.

## 5. Accelerating Power & Cooling Medium

The effective charge of a positively charged projectile in the retarding medium of a frictional cooling scheme can be absorbed into the accelerating power of the electric field. In effect, this makes the accelerating power dependent on the projectile's kinetic energy.

We reformulate here the requirements for frictional cooling stated in section 2: An equilibrium energy must be established by balancing energy loss with energy gain,

$$S(T_{\text{eq}}) = \frac{E}{\rho} \eta(T_{\text{eq}}). \quad (9)$$

At energies above  $T_{\text{eq}}$ , the stopping power must be greater than the accelerating power

$$S(T_{\text{eq}} + \epsilon) - \frac{E}{\rho} \eta(T_{\text{eq}} + \epsilon) > 0. \quad (10a)$$

And at energies below  $T_{\text{eq}}$  the accelerating power must be greater than the stopping power

$$\frac{E}{\rho} \eta(T_{\text{eq}} - \epsilon) - S(T_{\text{eq}} - \epsilon) > 0. \quad (10b)$$

The last two requirements can be combined to one statement about the slope of the stopping power relative to that of the accelerating power:

$$\left. \frac{dS}{dT} \right|_{T_{\text{eq}}} - \left. \frac{E}{\rho} \frac{d\eta}{dT} \right|_{T_{\text{eq}}} \equiv S'(T_{\text{eq}}) - \frac{E}{\rho} \eta'(T_{\text{eq}}) > 0. \quad (10c)$$

All three requirements can be met when

$$S' - S \frac{\eta'}{\eta} > 0. \quad (11)$$



	He	H <sub>2</sub>	Ne	C	N <sub>2</sub>	Ar	H <sub>2</sub> O	O <sub>2</sub>	Kr	Xe
without $\eta$	8.4	6.2	14.1	9.6	9.0	7.9	9.0	10.7	9.0	9.0 keV
with $\eta$	3.9	0.9	1.1		0.33	0.23	4.5	3.1		keV

Table 2: Maximum energy at which a stable equilibrium can be established in a frictional cooling scheme for  $\mu^+$  with and without accounting for effective charge for several stopping media. A blank entry means no equilibrium energy can be established.

Accounting for the muon’s effective charge greatly reduces the maximum energy at which the condition of equation (11) is met. Table 2 lists the cooling ranges for several materials with and without accounting for effective charge.

The effects of charge exchange processes also reduce the value of  $T'_{\text{eq}}$ , the maximum kinetic energy that can be decelerated to  $T_{\text{eq}}$ . This effect is illustrated in figure 4, which shows the frictional-cooling energy region of the stopping power of helium on  $\mu^+$ . Superimposed on the stopping-power curve are three electric-field accelerating powers: The black dashed line is the naive accelerating power of figure 1, with effective charge neglected, for a field strength 560 kV cm<sup>2</sup>/mg resulting in  $T_{\text{eq}} = 1$  keV. The lower red curve is the accelerating power for the same electric field strength, accounting for effective charge. The equilibrium energy is cut in half, but  $T'_{\text{eq}}$  remains the same. The upper red curve shows the accelerating power accounting for effective charge that results in  $T_{\text{eq}} = 1$  keV, which requires a field strength of 970 kV cm<sup>2</sup>/mg, and reduces  $T'_{\text{eq}}$  by a factor of two.

Achieving the desired equilibrium energy, accounting for effective charge, requires a greater electric field strength than is expected in the naive scheme. The field strength may in fact have to be an order of magnitude larger, depending on what the desired  $T_{\text{eq}}$  and the stopping medium are (figure 5). On the bright side, the relative slope of the stopping power is generally larger when effective charge is accounted for, perhaps causing (according to [4]) the final energy spread of a cooled beam to be smaller. As well, the stronger electric fields may reduce the spread caused by scattering.

We performed Monte Carlo simulations of the cooling of  $\mu^+$  beams with discrete charge exchange interactions, as well as simulations using the effective-charge approximation. These conformed to the calculations presented in figure 5 to within a few percent.

From the simulations we can calculate the spread of the beam energy around  $T_{\text{eq}}$  due solely to charge exchange interactions. Table 1 lists these spreads for  $\mu^+$  in helium at the same equilibrium energies cooled to in [4],

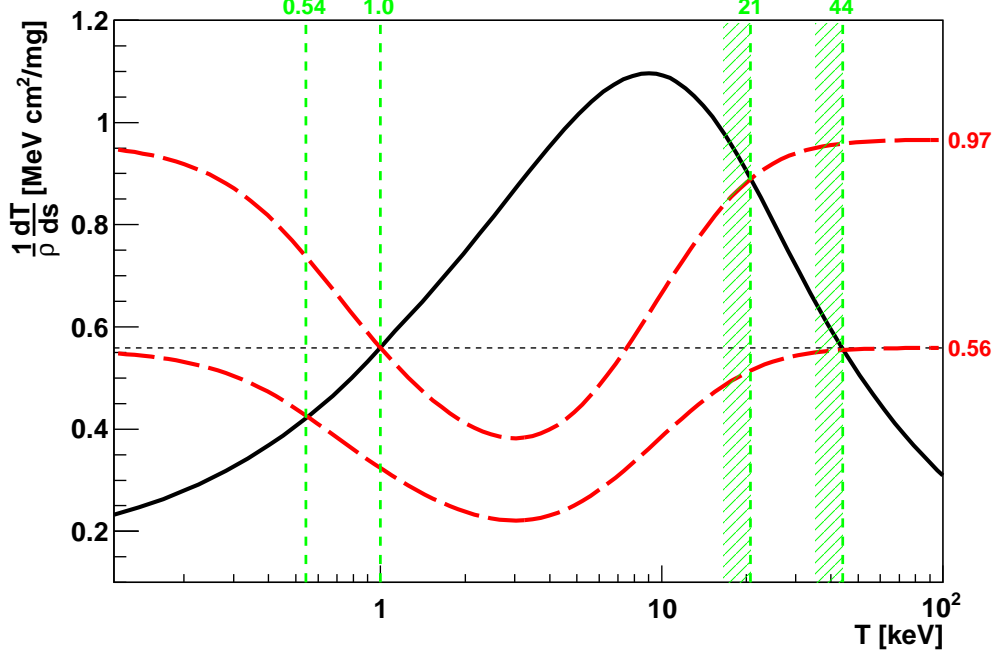


Figure 4: Stopping power of helium on  $\mu^+$  (solid) and accelerating power of a uniform constant electric field of strength  $E$  on  $\mu^+$  in helium with (large dashes, red) and without (small dashes, black) accounting for effective charge for two values of  $eE$  (as indicated on the right axis).

which looked at  $\mu^-$  in hydrogen. The spread due to charge exchange for  $\mu^+$  is smaller than the spreads due to scattering and straggling for  $\mu^-$ . A comparison using  $\mu^+$  in hydrogen is not possible because the maximum  $T_{\text{eq}}$  in  $\text{H}_2$  for  $\mu^+$  is 0.9 keV.

The choice of stopping medium is even further limited than the requirement that the relative slope of the stopping power be positive. This is illustrated by the example of oxygen, in which the relative slope of the stopping power is just barely positive over a small region of energies; but it is not sufficiently large to clearly establish an equilibrium energy.

Furthermore, at low energies, oxygen's stopping power is proportional to particle velocity,  $S \propto T^{\frac{1}{2}}$ , but its  $\eta$  is proportional to  $T^k$ , with  $k > \frac{1}{2}$ , causing the accelerating power to decrease below the stopping power at low energies. A particle that experiences a large loss of energy in one interaction—or one that scatters into a direction opposite that of the electric field—will not reaccelerate to  $T_{\text{eq}}$ , but rather continue decelerating to thermal energies and be lost to the cooling process. This would severely limit the use of such a

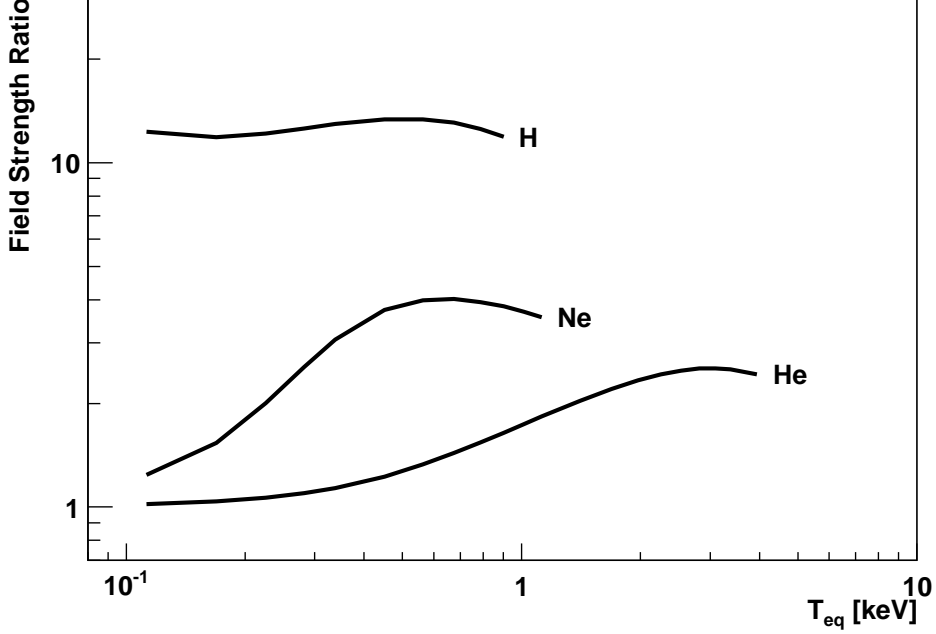


Figure 5: Ratio of electric field strength required to achieve the desired equilibrium energy accounting for effective charge to the field strength required without accounting for effective charge.

medium in a frictional cooling scheme.

The only viable media for a gaseous frictional cooling scheme for  $\mu^+$  with equilibrium energies at or above 1 keV are helium and water vapor. For  $T_{eq}$  just below 1 keV, hydrogen and neon also become viable; and for  $T_{eq}$  of a few hundred electron volts, argon and nitrogen are also viable.

## 6. Beam Neutralization & Foils

The frictional cooling experiment of [5] iterated energy loss and replacement by means of a series of moderating foils with electric fields between them. The experiment and a Monte Carlo simulation in [4] gave promising results for such a scheme for the cooling of negative muons. In both publications it was posited that the frictional cooling scheme used with  $\mu^-$  could also work with  $\mu^+$ ; more recently this idea has been revisited in [17] and [18]. However, the presence of charge exchange interactions greatly limits the yield for such a scheme; in fact, leading to a zero yield.

A foil-based frictional cooling scheme has the benefit of separating energy loss, occurring in the foils, from energy restoration, occurring between foils.

Since particles are reaccelerated in vacuum, the energy restoration depends on the charge state of the particle as it exits the foil. Those exiting in a neutral state are blind to the reacceleration field.

The four studies cited above used and simulated carbon foils in their frictional cooling schemes, choosing the reacceleration field strength to precisely compensate the energy lost in a foil by a particle at  $T_{\text{eq}}$ ; and assumed every particle exits every foil in a charged state. However, for positively charged particles, after exiting a foil at mean energy  $T_{\text{eq}}$ , a beam will be divided into two populations, a fraction  $f^+(T_{\text{eq}})$  in the  $\mu^+$  state and a fraction  $(1 - f^+(T_{\text{eq}}))$  in the Mu state. The  $\mu^+$  portion of the beam reaccelerates to  $T_{\text{eq}}$ , and upon exiting the next foil in the cooling series, its population fraction decreases further to  $(f^+(T_{\text{eq}}))^2$ . The Mu portion of the beam will not have its energy losses to the previous foil restored by the electric field and will exit the next foil at an energy below  $T_{\text{eq}}$ , where the chances of Mu atoms losing their electrons are even smaller. Furthermore, Mu atoms that have their electrons stripped off, must exit several foils in a row in the positive state in order to reaccelerate back to  $T_{\text{eq}}$ . As the beam passes through the array of foils it is neutralized and slowed down. Cooling becomes an impractical goal.

We performed a Monte Carlo simulation of exactly this mechanism. The foil density was chosen to match the simulations in [4] and the experiment in [5],  $5 \mu\text{g}/\text{cm}^2$  (25-nm-thick foils of  $2\text{-g}/\text{cm}^3$  amorphous carbon). Scattering and energy-loss straggling were neglected, since they would only worsen the beam neutralization described above. Figure 6 shows the yield<sup>4</sup> of the foil-based scheme as a function of the number of foils traversed for mono-energetic beams starting at 9 keV, the maximum  $T_{\text{eq}}$  possible, and 4 keV, the  $T_{\text{eq}}$  used in [4]. After a handful of foils, the yield falls off exponentially with the number of foils traversed. After passing through the first foil and energy restoration, the mean energy of the beam is greatly reduced from  $T_{\text{eq}}$  and the energy spread is greatly enlarged. The mean energy continues to fall with each successive foil.

We also simulated a scheme in which the foils are coated with frozen noble gas to increase the fraction of particles exiting them in the positive charge state. This is inspired by the scheme for the production of low-energy muons from a surface muon beam at the Paul Scherrer Institute (PSI), which uses frozen argon and krypton [19]. Neither argon nor krypton coatings

---

<sup>4</sup>In the simulation, tracking of a particle is terminated when it does not have sufficient kinetic energy to pass completely through a single foil according to [6]. The yield is thus defined as the fraction of muons surviving passage through the foil.

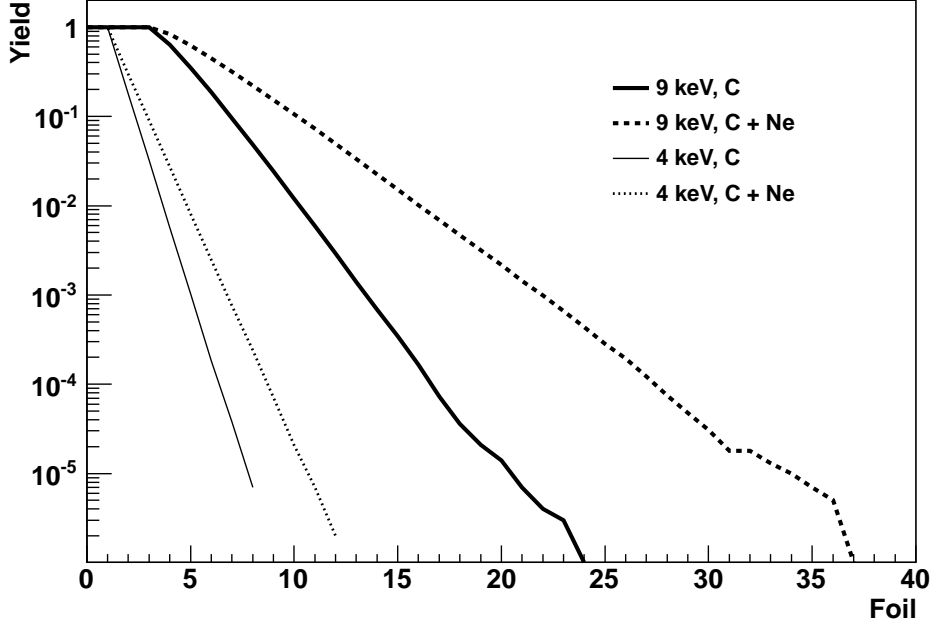


Figure 6: Yield of  $\mu^+$  in carbon-foil frictional cooling schemes as a function of number of foils traversed after reaching  $T_{\text{eq}}$ , for both naked foils and frozen-neon-coated foils.

improve the beam neutralization. A neon coating marginally slows beam neutralization (shown in figure 6), but does not prevent the degradation of the beam energy. Moreover, we simulated the charge-exchange effects of the coatings but neglected their impact on energy loss. This assumes that the coatings are nanometers thin; however, the coatings used at PSI are a much thicker 200 – 300 nm. Such thicker coatings would hasten beam loss.

The scheme of [17], also based on carbon (graphite) foils, requires the beam to pass through order-100 foils at the equilibrium energy. A beam of positively charged muons (or protons) would be unable to survive such a scheme.

## 7. Conclusion

Muon collider schemes employing frictional cooling are a viable option for collision of multi-TeV lepton beams. Several articles have been published with analytical and experimental results for frictional cooling of negatively charged particles. Many of these articles have conjectured that the results for positively charged particles will be the same as for negatively charged ones,

and schemes for the cooling of positive particles have been proposed. A key group of physics processes involved in the slowing down of positive particles—those changing the charge state—has been neglected in these studies. We found that accounting for these processes significantly alters the results for positive particles from those for negative ones: The choice of cooling medium is greatly limited, such that helium gas becomes the only viable medium; with foil-based schemes completely ruled out. The range of equilibrium energies for the cooled beam is also greatly limited, with a maximum possible energy of approximately 4 keV for  $\mu^+$  (36 keV for protons). And the electric field strength required to bring a beam of positive particles to an equilibrium energy is significantly greater than the strength required to bring a beam of negative ones to the same energy.

## References

- [1] M. M. Alsharo *et al.*, Phys. Rev. ST Accel. Beams **6**, 081001 (2003).
- [2] C. Ankenbrandt *et al.*, Fermilab Report No. TM-2399-APC, 2009.
- [3] H. Abramowicz, A. Caldwell, R. Galea, and S. Schlenstedt, Nucl. Instr. and Meth. A **546**, 356 (2005).
- [4] M. Mühlbauer, H. Daniel, and F. J. Hartmann, Hyperfine Interact. **82**, 459 (1993).
- [5] M. Mühlbauer *et al.*, Nucl. Phys. B **51A**, 135 (1996).
- [6] Stopping powers and ranges for protons and alpha particles, 1993, Bethesda, USA: ICRU (1993) 286 p. (ICRU report: 49).
- [7] B. H. Bransden and C. Forster, J. Phys. B-At. Mol. Opt. **23**, 115 (1990).
- [8] M. Agnello *et al.*, Phys. Rev. Lett. **74**, 371 (1995).
- [9] P. Sigmund and A. Schinner, Eur. Phys. J. C. **15**, 165 (2001).
- [10] D. Neuffer, Part. Accel. **14**, 75 (1983).
- [11] V. V. Parkhomchuk and A. N. Skrinsky, AIP Conf. Proc. **352**, 7 (1996).
- [12] U. Fano, Ann. Rev. Nucl. Part. Sci. **13**, 1 (1963).
- [13] J. F. Ziegler, J. P. Biersack, and M. D. Ziegler, *The Stopping and Range of Ions in Matter* (SRIM Co., 2008).

- [14] S. K. Allison, Rev. Mod. Phys. **30**, 1137 (1958).
- [15] Y. Nakai, T. Shirai, T. Tabata, and R. Ito, Atom. Data Nucl. Data **37**, 69 (1987).
- [16] A. E. S. Green and R. J. McNeal, J. Geophys. Res. **76**, 133 (1971).
- [17] T. J. Roberts and D. M. Kaplan, Particle Refrigerator, in *PAC09*, 2009.
- [18] D. M. Kaplan, Muon Cooling and Future Muon Facilities: The Coming Decade, in *DPF09*, 2009.
- [19] E. Morenzoni *et al.*, Phys. Rev. Lett. **72**, 2793 (1994).